Evaluation of bone regeneration enhancement by in-vivo study using MAPTMS.

Mohamed S. El-Khooly *

Physics Department, Faculty of Science, New Valley University, El-Kharja 72511, Egypt

Doi: 10.21608/nujbas.2025.380531.1043

Article information: Submit Date 30 April. 2025; Revise Date 25 June 2025; Accept Date 9 July 2025

Abstract

In this study, we employ 3-methacryloxypropyl trimethoxy silane (MAPTMS), an organic substance made using the sol-gel technique, which has been assessed as a bioactive bone substitute. An ethanol/water solution was used to achieve hydrolysis and condensation. The functional groups, crystal structure, and morphology were confirmed employing several techniques, including infrared spectroscopy, X-ray diffraction, and scanning electron microscopy. The bioactivity of this sample was studied via in-vivo test by implanting the samples inside the tibia of rats for 1, 4, and 8 weeks. Results showed that the grafting materials used in repairing the bone defects do not cause histopathology with the peripheral osseous tissue because all animals lived without experiencing any local or general issues. The results also showed, after comparing the control sample (a group of rats) to which the same operation was performed without MAPTMS, that the group to which MAPTMS was applied had better bone tissue healing and recovery than the control sample.

Keywords: Biomaterials, In-vivo, Sol-gel, Bone regeneration, MAPTMS.

Introduction

The biocompatibility of transplanted materials is a critical component in the bone healing process. As evidenced by the absence of allergic, poisonous, or inflammatory responses, it suggests that the live tissue is responding appropriately to the materials **[1], [2]**. Organic materials tend to trigger a strong immune response but usually break down well in the body and have better qualities than many inorganic compounds. A combination of organic and inorganic compounds can be used, as these compounds are manufactured through a hybridization process in which two or more components, usually organic and inorganic, are combined. Sol-gel technology allows the incorporation of polymers of different natures at relatively low temperatures, which keeps the organic materials from coagulating or burning **[3]**. Straightforward to utilize in medical environments, osteogenic, biocompatible, resorbable, capable of supplying structural support, able to act as a drug carrier, and offering a reasonable rate-benefit ratio **[4]**. To tackle specific challenges in human clinical practice, any of these traits may be preferred above the others **[5], [6]**. Autografting and allografting cancellous bone are suggested in numerous therapeutic applications, however some issues, such as pain and infection, along with the restricted autograft supply, might result from these treatments **[7], [8], [9]**. Furthermore, allografting adds the danger of illness and/or infection, and it might result in the entire loss of bone inductive element **[10], [11]**. In addition, in large defects, the graft in the body could be resorbed before osteogenesis is complete **[12]**. Avoid the risk of transmission of disease and the economic cost of allografts, in addition to preventing self-morbidity in bone autografts, the utilization of innovative synthetic bioactive materials offers a growing prospect for therapeutic applications in human practice **[13]**. Furthermore, our studies have shown the usefulness of glass-ceramic and sol-gel glass in vivo in curing restricted bone abnormalities **[14]**. The findings indicate that MAPTMS is suitable for bone replacement or repair (filling voids or covering implant surfaces), as well as for certain reasons in growth plate surgery. To determine if these materials can be employed for extended bone defect treatment, we evaluated the in vivo behavior of a sol-gel MAPTMS as bone replacements in critical bone defect repair **[4]**. We can produce at room temperature by using the sol-gel technique **[5], [6]**. Inorganic and organic sol-gel materials offer a variety of applications in domains such as optics, ionics, electronics, energy, mechanics, and biology **[7], [8]**. catalysis, separation, and sensing electrochemistry **[15], [16], [17], [18], [19], [20], [21], [22], [23], [24], [25], [26], [27], [28], [29]**. Corrosion-resistant coatings and useful functional smart materials **[7], [8], [30], [31]**, or biomedical and biomaterials applications **[8]**. In this work, we prepared gamma-methacryloxypropyl trimethoxy silane (MAPTMS) by the sol-gel method. Extensive information is available on the binding of 3-methacryloxypropyltrimethoxysilane to a wide range of inorganic materials, including, for example, glass, silica,

* Corresponding authors: M.s.elkhooly@sci.nvu.edu.eg

alumina, and titanium, making it a good catalyst for its bonding to natural bone, which is composed of a crystalline mineral fraction [32]. The organic silane precursor, such as MAPTMS, contains organic groups that can function as network modifiers. Depending on the type of organic group used, the presence of these modifiers offers the modified silicon network additional features (such as hydrophobicity and flexibility) [33]. The hydrolyzed silanol groups (Si-OH) can interact with hydroxyl groups (OH) on metal or inorganic surfaces by forming hydrogen bonds, which are then condensed to produce oxane bonds [34], [35].

The aim of this study is to use the MAPTMS as a polymer a bone growth stimulant with calcium chloride for greater biocompatibility and allow the regenerated bone at the site of healing to form holes that help in supplying the capillaries, which increases with the gradual dissolution of the polymer, and apply this practically inside the leg of mice and compare it to healing without that substance MAPTMS .By preparing an organic MAPTMS silane precursors, We predict that this design will stimulate the production of bone. Histopathological analysis and x-ray radiography have been employed to confirm the accuracy of this idea.

Materials and Methods

i. Sample preparation:

Synthesis of MAPTMS (powder): By dissolving the proper amounts of (MAPTMS) and distilled water in ethanol was created using the sol-gel method. For twenty minutes, the MAPTMS/ethanol/H_2O mixture swirled at room temperature. In order to prevent phase separation, after that, hydrochloric acid was added to accomplish acid hydrolysis. For ten more minutes, the MAPTMS/ethanol/H_2O/HCl mixture swirled at room temperature. Lastly, to boost the sample's bioactivity, 0.2 grams of calcium chloride were added to the solution. At room temperature, the mixture was stirred for ten minutes as well. The sol-gel transition (condensation process) was then obtained by stirring it for four hours at 50˚C. It was reported that when the beaker is tilted, the flow ceases at the gelation condition. In a drying oven, the gel that formed was dried for six days at 120˚C. The selected samples were crushed (milled) in an agate mortar [36]. The preparation steps are shown in **Fig. 1**.

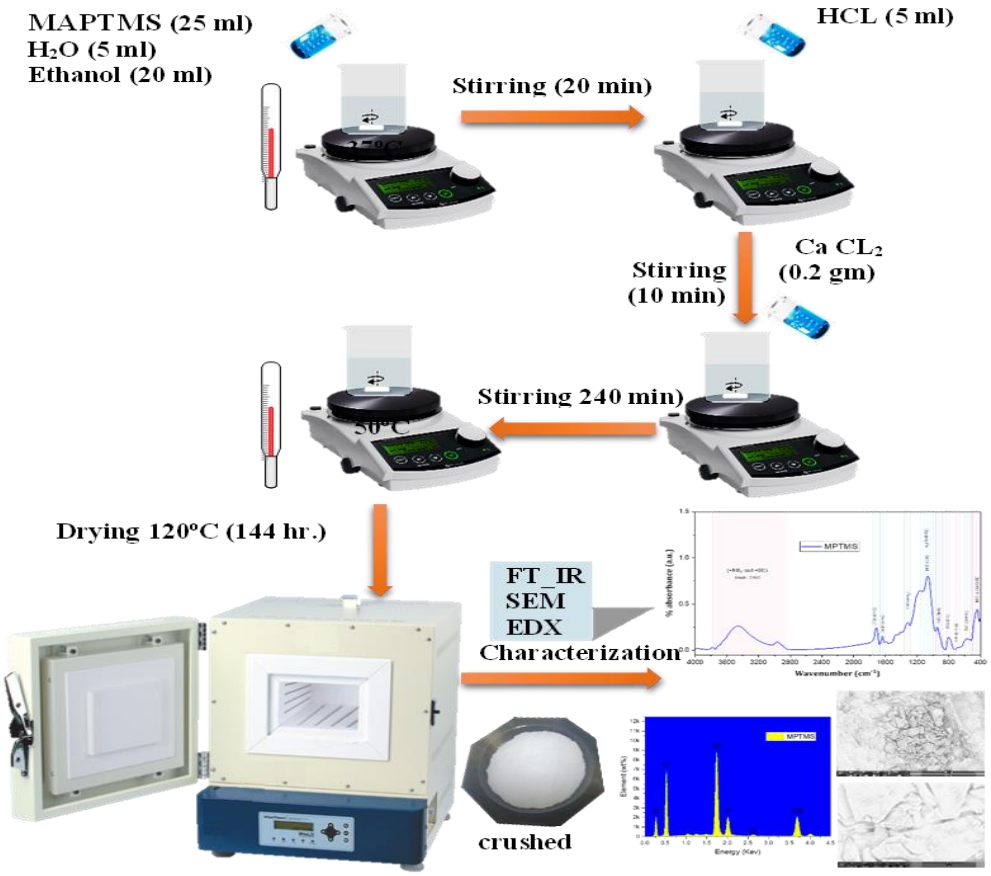

Fig. 1. Flowchart of preparation of MAPTMS-$CaCl_2$ steps.

The MAPTMS basic theoretical aspects.
Appearance and Smell of 3-(Methacryloyloxy)propyl trimethoxysilane is a pale yellow to colorless, clear, and transparent liquid with a slightly rosin-like odor. The density (ρ) of MAPTMS is 1.055g/cm3, the boiling point (at 760mmHg) is 255°C, the molecular formula is C10H20O5Si, number of atoms is 36, and the molecular weight 248.35 Da. Atoms are shown as ball-and-stick in a representation with standard colors and chemical composition structure 2D in the **Fig. 2**.

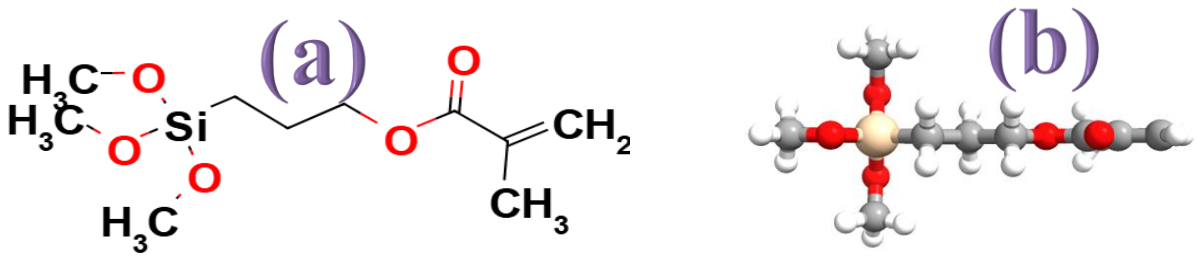

Fig. 2. shows the MAPTMS (a) Chemical composition structure 2D, (b) model is a Quick Submit entr

ii. In-vivo Study: Operation
placed within the rats' tibia for 1, 4, and 8 weeks using an in-vivo study: Afterward, several characterization methods were used to examine the sample's bioactivity in comparison to the control.

a) Preoperative preparation technique:

Aseptic surgery was performed on the surgical site, which included the tibia, the lower part of the hind limb. Hair was clipped and shaved to prepare the skin, and as seen in Fig. (3-a), at least three surgical scrubs using cotton soaked in povidon iodine were administered for 10 minutes. During the procedure, double medical gloves, stockinets, and towels were employed.

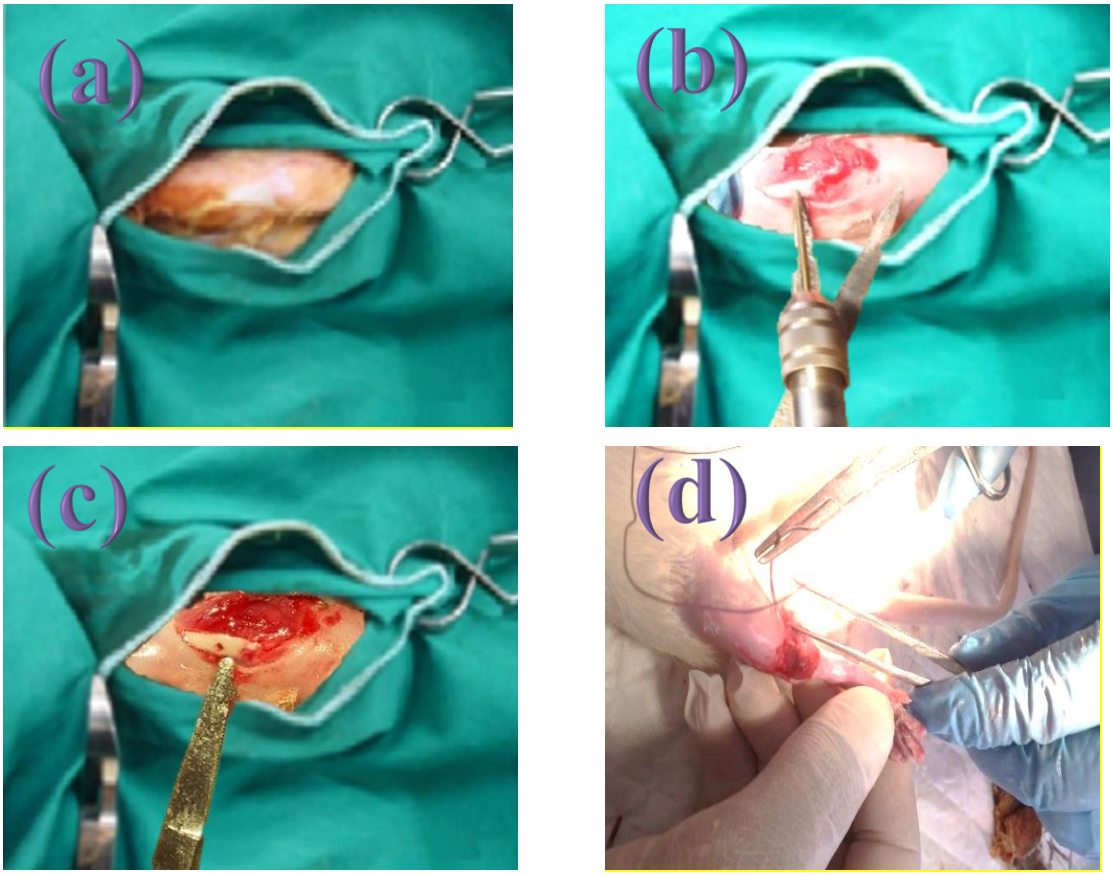

Fig.3. (a,b,c) Surgical procedures, implant was handled from its site, **(d)** suture of the skin and tissues.

b) Surgical procedures

Experiments and surgery were carried out at MRC Ain Shams University's Medical Research Center. According to institutional guidelines, the surgical procedures were carried out in accordance with ethical standards for animal research. The animals were put to sleep using ketamine hydrochloride injection USP, which contains 50 mg of ketamine per milliliter and is administered intraperitoneally at a dose of 40–45 mg/kg body weight. Betadine (povidone-iodine) solution was used to prepare the surgical site after it had been shaved **Fig. 3. (a)**. Using a mucoperiosteal elevator, the bone was exposed after an incision of about 3 cm in length was created on the medial surface of the tibia, extending through the periosteum. The implant was manually removed from its location.

A low-speed electric drill was used to drill a 2 mm hole in the tibia **Fig. 3. (b)**, It was then cleansed using a sterile saline solution. To avoid scorching the bone and washing away bone fragments, the drilling procedure was carried out at a slower rate and thoroughly watered. The hole was expanded into the cancellous bone through the cortex. The sample powder was poured into the hole **Fig. 3. (c)**. Lastly, saline was used to irrigate the operative site. Using polyglycolic acid suture, the fascia and skin were moved and sutured (the skin and subcutaneous tissues were sutured to encapsulate the samples) **Fig. 3. (d)**. Following surgery, dermotracin spray was administered as an antibiotic, and the rat was also given an injection of the drug. In order to decrease the chemicals in the body that generate pain and inflammation, voltaren, a nonsteroidal anti-inflammatory medicine, was finally put into the rat. On the seventh day, an X-ray was taken to make sure the limb was positioned correctly.

c) Histological analysis [37].

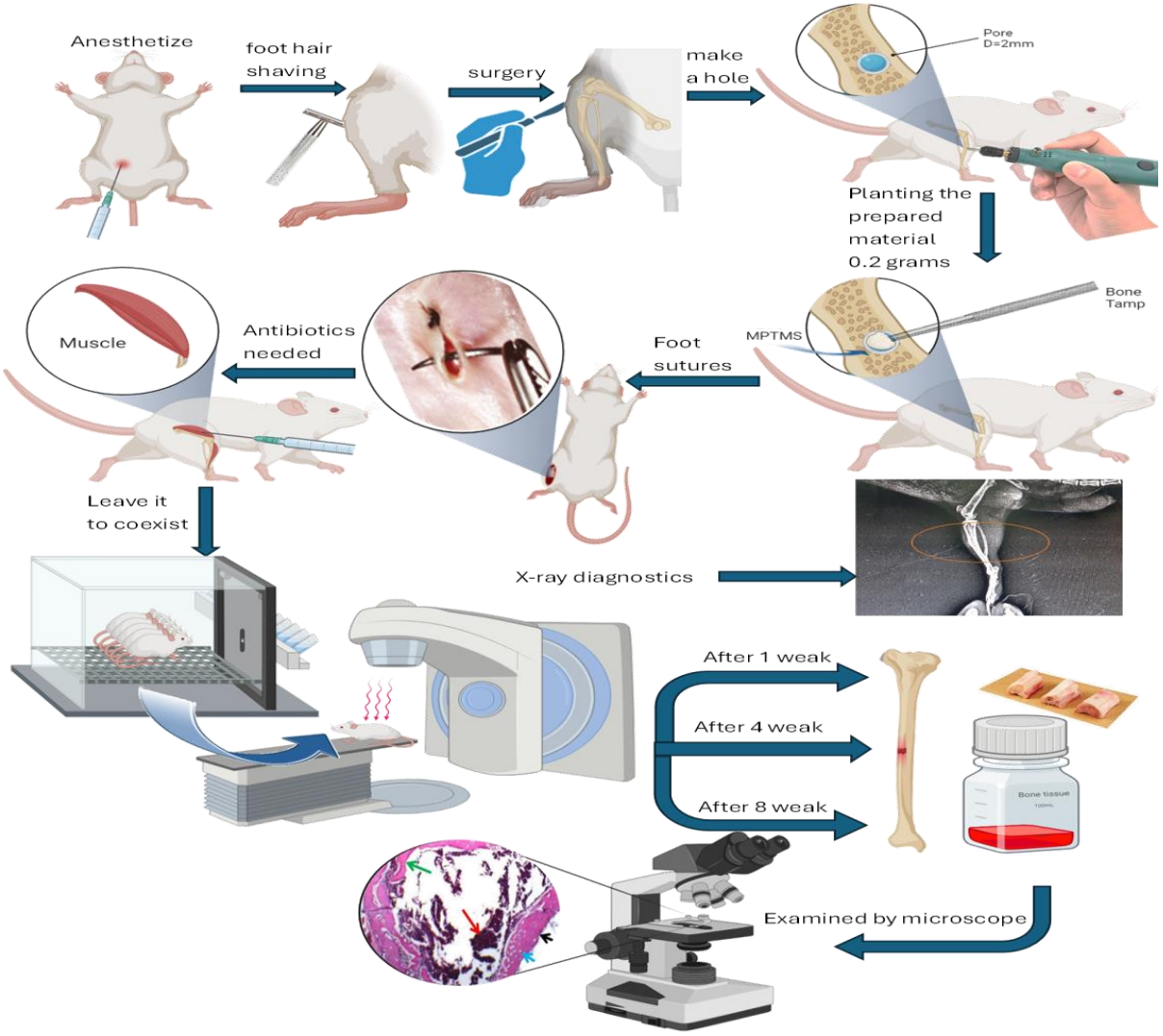

Fig. 4. graphical abstract for surgical, characterizations and histological processes steps.

After ethical approval of the study protocol by the Ethics Committee Faculty of Medicine, Al-Azhar University (No. of approval: 2021121135). The animals were slaughtered under general anesthesia on the 7th, 30th, and 60th days following the surgeries. A portion of the tibia was resected. Tissue samples were embedded in paraffin slices.

Preparation of paraffin sections:

- In formic acid, decalcification occurs.
- Dehydration: achieved by increasing alcohol levels:
  - 70% alcohol: 90 minutes.
  - 1.5 hours with 90% alcohol.
  - Total alcohol (Absolute): three hours.
- Cleaning: For four hours, the specimens were cleaned in xylene.
- Infiltration: After being cleansed, the specimens were impregnated in three grades of soft, pure paraffin at 56 °C for an hour each.
- Imbedding: Finally, the specimens were in hard paraffin wax at 58 °C.
- Cutting: For histological analysis, paraffin slices with a thickness of 5–6 micrometers were cut.
- Hematoxylin and Eosin staining (H & E)
- Covered and mounted in DPX

A light microscope was used to analyze the status of the surrounding tissue, the presence as well as the position of fibrous tissue, and the hilling of bone cells (**nikon, eclipse, 80i, Japan**). Newly created bone with thickness, density, degree of remodeling, remodeling fibrosis (Sharpey's fibers), and angiogenesis response surrounding the bone cement were rated and scored in randomly chosen fields at different magnifications. **Fig.4.** provides a summary of each stage along with drawings.

Results and Discussion

a) Characterization Techniques

i. FT-IR examination.

Fig.5. Shawn Fourier transforms of all the functional groups that comprise the chemical structure were revealed by the material's infrared analysis, confirming the preparation's safety and the materials' purity and suitability for research. The silica network's primary unique bands were apparent in the MAPTMS FTIR spectra. The band discovered close to 445 cm^{-1} is attributed to out-of-plane bending of Si-O-Si [38]. The band at 1066 cm^{-1} is returned to C-H between 1080 and 1140 cm^{-1} **[38]**. However, the C=C group of the methacrylate groups from the organic precursor is responsible for the band at 1639 cm^{-1} **[39]**. The vibration bands at 2940 and 2837 cm^{-1}, which are indicative of the symmetric and asymmetric C-H functional bond, were detected on MAPTMS surface that are silanized. The primary functional groupings' FTIR maps are displayed: N-H at wavenumber 3437 cm^{-1} **[38]**. The FTIR signal at 3434.29 cm^{-1} was mainly due to the presence of OH stretching with free water or hydroxyl groups on the MAPTMS surface **[40]**.

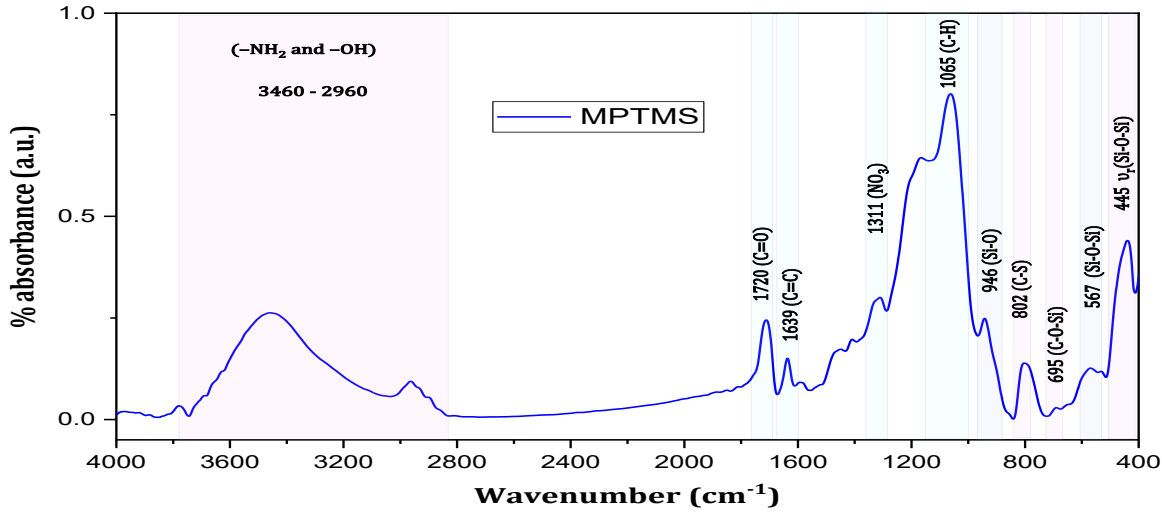

Fig. 5. FT-IR spectrum of MAPTMS.

ii. Energy dispersion of X-rays (EDX) with scanning electron microscopy (SEM).

Based on the findings of an examination using scanning electron microscopy, as shown in **Fig. 6. (a)** at 500x magnification, the sample surface was smooth with some cracks, clearly visible in **Fig. 6. (b)** at 3000x magnification. Based on their proportions, energy dispersion of X-ray (EDX) data, as shown in **Fig. 6. (c)**, confirmed the correct amounts of each chemical element that constituted the material's chemical composition.

iii. X-Ray radiography

Fig. 6. (d) show a lateral image of the tibia treated with specimen MAPTMS after one week from performing the operation. X-Ray radiography was used to ensure defects in the right tibia bone of rats. X-ray shows increasing in cortical thickness due to the presence of the sample (MAPTMS) which acted as an osteoconductive and osteoinductive material that enhanced new bone formation at the defect site because it is a good bioactive material.

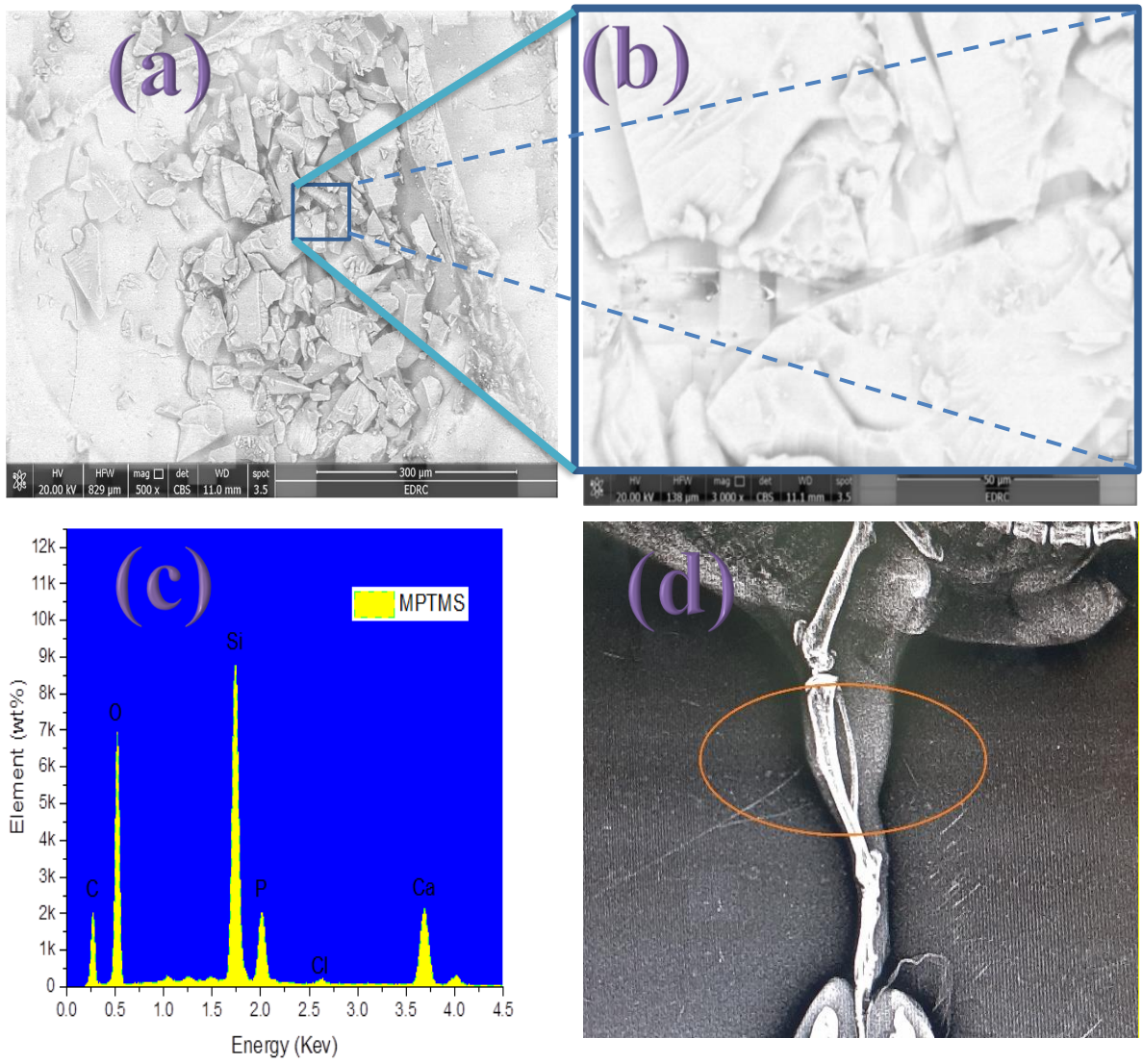

Fig. 6. (a,b) SEM images for MAPTMS at 500,3000x, **(c)** the EDX spectrum, and **(d)** the image of x-ray after 1week.

b) Histopathological results:

All mice that had surgery lived for two months after the operation process; none indicated infection at the surgical site or immunological sensitive responses, such as inflammation, indicating the biocompatibility of the implant tissue under study. Histological analysis also showed that the implant had good osteoinductive potential compared to the control implant. The presence of the MAPTMS accelerated healing time and stimulated bone formation. It also allowed for the formation of small holes, which increased the capillary supply to the surgical site and

increased the number of osteoblasts and osteoclasts, enabling them to take on a regular crystalline shape, making the resulting bone tissue more solid and crystalline.

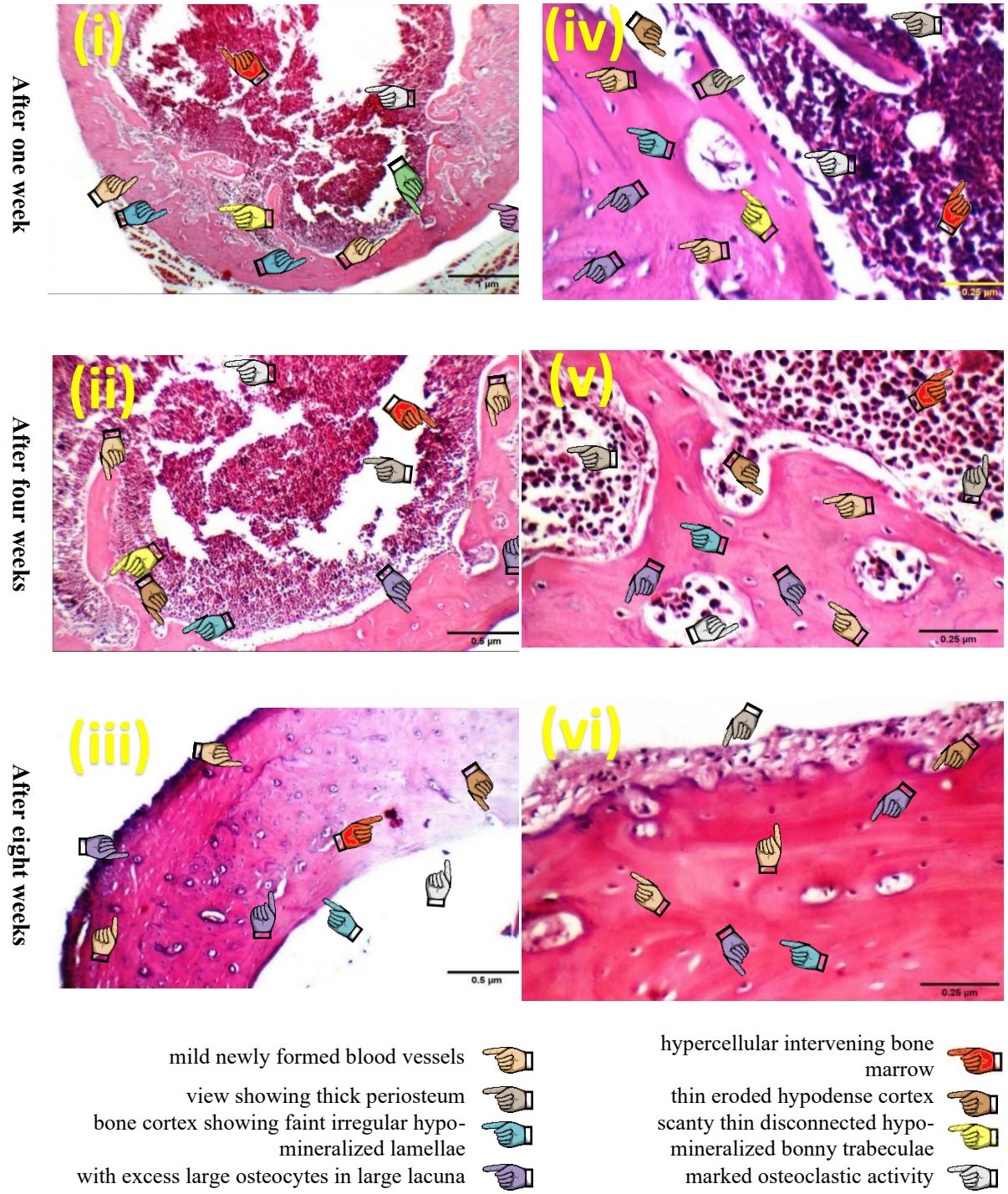

Fig. 7. Histological MAPTMS -Treatment **(i)**(H&E X 100), **(iv)**(H&E X 400) after one week, **(ii)** (H&E X 200), **(v)** (H&E X 400) after 4 weeks, **(iii)** (H&E X 200), **(vi)** (H&E X 400) after 8 weeks.

The bones of the mice are treated by MAPTMS **Fig. 7. (i)** after one week, **Fig. 7. (ii)** after four weeks, and **Fig. 7. (iii)** after eight weeks at small magnifications (H&E X 100, H&E X 200, H&E X 200) respectively are show relatively thick cortex with regular dense lamellae parallel to small osteocytes in small lacuna, mild inactive osteoblastic rimming and marked newly formed blood vessels and thin dense bonny trabeculae with mild inactive osteoblastic rimming, and hypercellular intervening bone marrow.

Higher magnifications reveal these findings more clearly in **Fig. 7. (iv)** after one week, **Fig. 7. (v)** after four weeks, and Fig. **Fig. 7. (vi)** after eight weeks at a large magnification (H&E X 400).

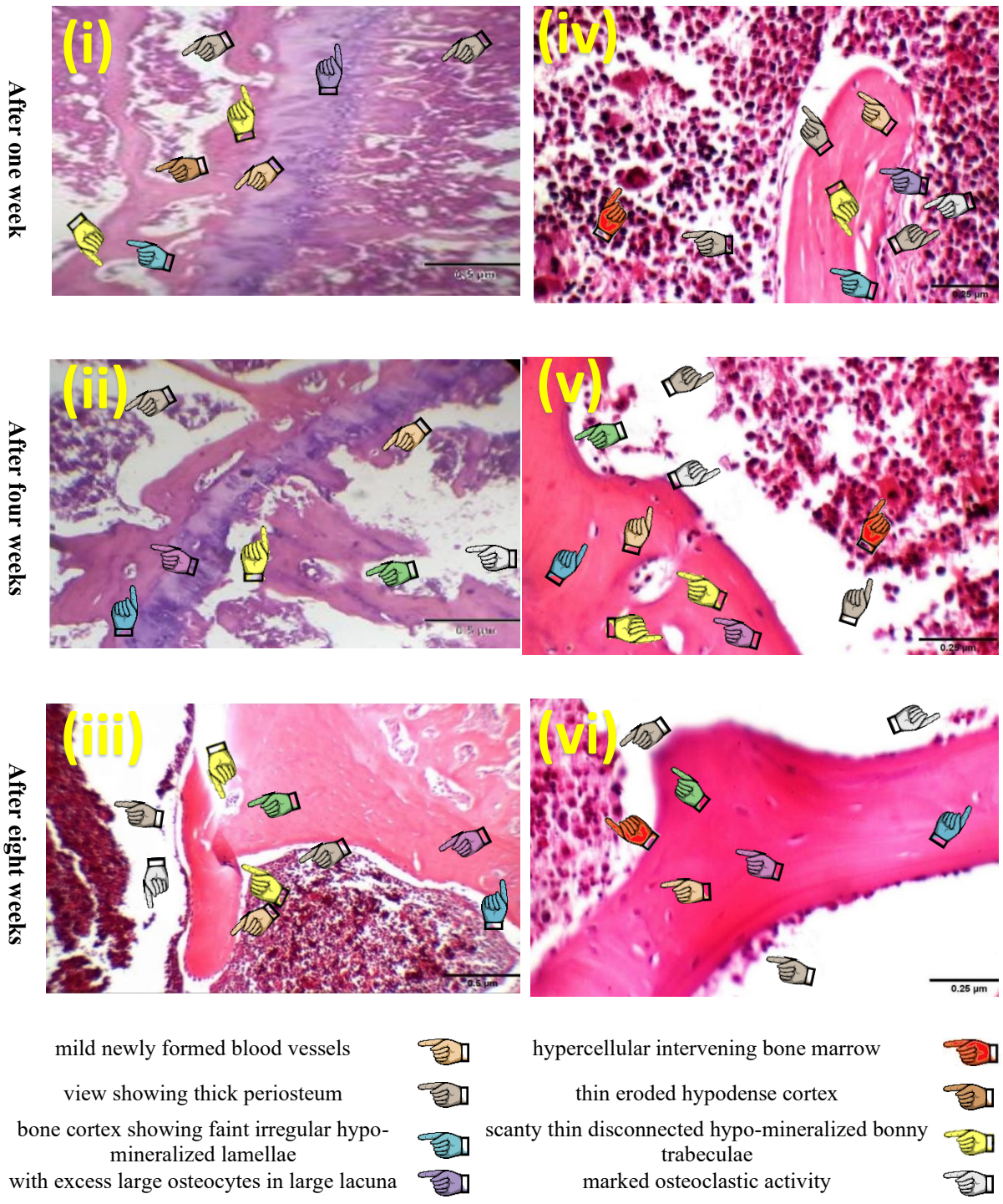

Fig. 8. Histological non -Treatment (control) **(i)**(H&E X 200), **(iv)** (H&E X 400) after one week, **(ii)** (H&E X 200), **(v)** (H&E X 400) after 4 weeks, **(iii)** (H&E X 200), **(vi)** (H&E X 400) after 8 weeks.

The bone Control mice's are not-treatment **Fig. 8. (i)** after one week, **Fig. 8. (ii)** after four weeks, and **Fig. 8. (iii)** after eight weeks are show thick periosteum, thin destructed and eroded hypodense cortex with faint irregular hypo-mineralized lamellae, excess large osteocytes in large lacunae, marked osteoclastic activity with mild inactive osteoblastic rimming and mild newly formed blood vessels, scanty thin disconnected eroded hypo-mineralized bonny trabeculae with excess large osteocytes in large lacunae, and hypercellular intervening bone marrow.

Higher magnifications reveal these findings more clearly in **Fig. 8. (iv)** after one week, **Fig. 8. (v)** after four weeks, and **Fig. 8. (vi)** after eight weeks at a large magnification (H&E X 400).

Table 1. Density, Lamellae, osteocytes and Osteoblasts in Cortex and Trabecula.

	Cortex					Trabecula			
	Density	Lamellae	Osteocytes	Osteoblasts	BV	Density	Lamellae	Osteocytes	Osteoblasts
Control	1	1	0	1	0	2	1	0	1
MAPTMS	2	2	2	0	2	2	2	2	0

Table 2. meaning of numerical values of Lamellae, Osteocytes, Osteoblasts, BV in Cortex.

Cortex	**0: Hypodense**	**1: Irregular density**	**2: Dense**
Lamellae	**0: Irregular faint**	**1: Irregular dense**	**2: Regular dense**
Osteocytes	**0: Excess large**	**1: Few large**	**2: Small**
Osteoblasts	**0: Mild inactive**	**1: Mild active/ moderate inactive**	**2: Moderate/marked active**
BV	**0: Mild newly formed**	**1: Moderate newly formed**	**2: Marked newly formed**

The major goal of this work was to study the effect of increasing organic precursor (MAPTMS-$CaCl_2$) on biocompatibility and bone regeneration in rats. No histology sections appeared to exhibit any evidence of inflammation or necrosis around any of the implants tested. The same conclusion that was reached by the in vivo test was supported by the discovery that increasing the MAPTMS increases angiogenesis, which raises the blood supply and increases the delivery of minerals, which raises the density of newly formed bone, and increases the delivery of nutrients to bone cells, which increases their growth and development. The values in **Table 1.** illustrate these results, and the interpretation of the numbers indicated in this table is explained in **Table 2**.

Fig. 9. Illustrate a comparison in Cortical and trabecular thickness in (MAPTMS, control) samples. Also, cortical and trabecular thickness in rats treated with (MAPTMS) for one week is higher than in rats (Control) for two months. This result confirms that, (MAPTMS) decreases the time of formation of cortex and trabecula in bone.

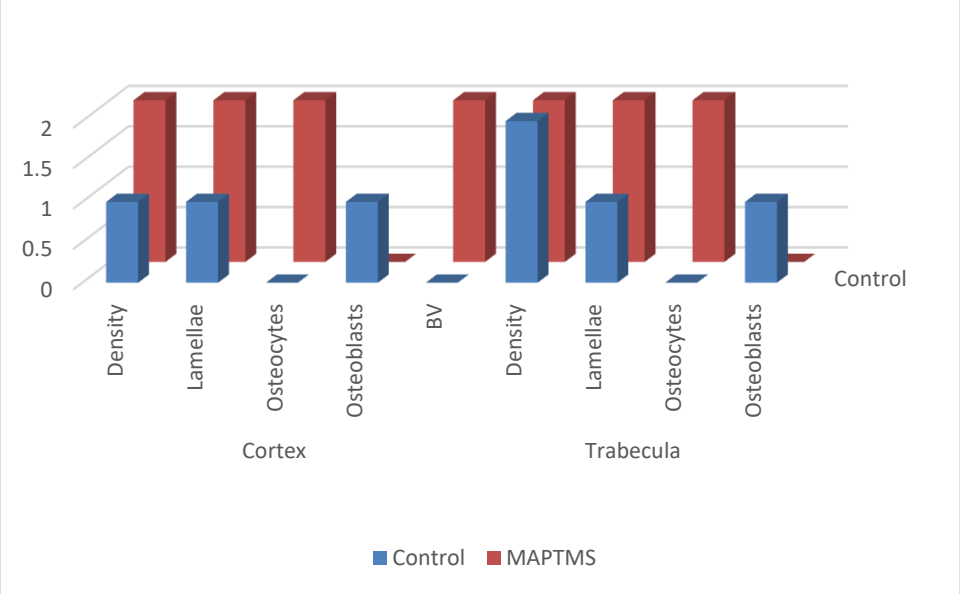

Fig. 9. Comparison in Cortical and trabecular thickness in (MAPTMS, control) samples

Conclusion

Silane-based materials (MAPTMES) with calcium chloride for greater biocompatibility were synthesized successfully via sol-gel method. The bioactivity of these samples was investigated by implanting the samples inside the tibia of rats for 1, 4 and 8 weeks. It appears that all animals lived without any local or general issues, indicating that the grafting materials placed in bone defects do not lead to histopathology with the peripheral osseous tissue.

• By functioning as an osteoconductor and bone stimulator, MAPTMS is a beneficial bioactive compound that encourages the formation of new bone at the healing site. Because of this, X-ray imaging showed an increase in cortical thickness.

• According to the histopathological findings, the MAPTMS sample's higher levels of organic precursors promoted angiogenesis, which in turn raised blood flow. This, in turn, improved mineral delivery, raised the density of newly formed bone, and improved the delivery of nutrients to bone cells, which in turn promoted bone cell growth and development. Additionally, mice treated with MAPTMS for one week had thicker cortical and spongy tissue than mice treated with the control sample for two months. This finding demonstrates that MAPTMS shortens the time needed for the formation of bone's cortex and spongy tissue.

Conflict of Interest

None.

Declaration of Funding

No funding was received for this study

References

[1] K. Marycz, J. Krzak, W. Urbański, and C. Pezowicz, "In vitro and in vivo evaluation of sol-gel derived TiO2 coatings based on a variety of precursors and synthesis conditions," *Journal of Nanomaterials,* vol. 2014, no. 1, p. 350579, 2014.

[2] A. S. A. Raboh, M. S. El-khooly, and M. Y. Hassaan, "Bioactivity and drug release study of dexamethasone loaded bioglass/Chitosan composites for biomedical applications," *Journal of Inorganic and Organometallic Polymers and Materials,* vol. 31, pp. 2779-2790, 2021.

[3] V. S. Gomide, A. Zonari, N. M. Ocarino, A. M. Goes, R. Serakides, and M. M. Pereira, "In vitro and in vivo osteogenic potential of bioactive glass–PVA hybrid scaffolds colonized by mesenchymal stem cells," *Biomedical materials,* vol. 7, no. 1, p. 015004, 2012.

[4] J. Gil-Albarova *et al.*, "The in vivo behaviour of a sol–gel glass and a glass-ceramic during critical diaphyseal bone defects healing," *Biomaterials,* vol. 26, no. 21, pp. 4374-4382, 2005.

[5] D. Chattopadhyay and D. C. Webster, "Hybrid coatings from novel silane-modified glycidyl carbamate resins and amine crosslinkers," *Progress in Organic Coatings,* vol. 66, no. 1, pp. 73-85, 2009.

[6] A. Kayan, "Inorganic-organic hybrid materials and their adsorbent properties," *Advanced Composites and Hybrid Materials,* vol. 2, pp. 34-45, 2019.

[7] G. Schottner, "Hybrid sol− gel-derived polymers: applications of multifunctional materials," *Chemistry of materials,* vol. 13, no. 10, pp. 3422-3435, 2001.

[8] C. Sanchez, B. Julián, P. Belleville, and M. Popall, "Applications of hybrid organic–inorganic nanocomposites," *Journal of materials chemistry,* vol. 15, no. 35-36, pp. 3559-3592, 2005.

[9] A. Abd raboh, M. El-khooly, and M. Hassaan, "Preparation of Bioglass/Chitosan Composite incorporated with Dexamethasone by Sol-gel Method," *Egyptian Journal of Biomedical Engineering and Biophysics,* vol. 0, no. 0, pp. 9-22, 2019, doi: 10.21608/ejbbe.2019.14005.1025.

[10] M. El-Khooly, A. Abdraboh, A. Bakr, and K. Ereiba, "Bioactivity and mechanical properties characterization of bioactive glass incorporated with graphene oxide," *Silicon,* vol. 15, no. 3, pp. 1263-1271, 2023.

[11] M. S. El-Khooly, "Drug Delivery of Corticosteroids," in *Updates on Corticosteroids*: IntechOpen, 2022.

[12] M. S. El-khooly, A. M. Bakr, and K. T. Ereiba, "Preparation of a Mixture of Bioglass/Sodium Alginate Doped with Silver Incorporated with Graphene Oxide," *Egyptian Journal of Biomedical Engineering and Biophysics,* vol. 24, no. 1, pp. 1-12, 2023.

[13] A. S. Abdraboh, A. M. Bakr, and K. T. Ereiba, "Fabrication and characterization of silver-substituted bioactiveglass incorporated with sodium alginate and graphene oxide," *Materials Chemistry and Physics,* vol. 301, p. 127716, 2023.

[14] M. El-khooly, A. A. Abdel-Aal, A. E. Mekky, A. Al-esnawy, and A. Abdraboh, "Tenoxicam-loaded Bioglass/Polyvinyl alcohol composites for biomedical applications: In-vitro study," *Materials Chemistry and Physics,* p. 130526, 2025.

[15] B. Casal, E. Ruiz-Hitzky, M. Crespin, D. Tinet, and J. Galvan, "Intercalation mechanism of nitrogenated bases into V 2 O 5 xerogel," *Journal of the Chemical Society, Faraday Transactions 1: Physical Chemistry in Condensed Phases,* vol. 85, no. 12, pp. 4167-4177, 1989.

[16] E. Ruiz-Hitzky, P. Aranda, B. Casal, and J. C. Galvan, "Nanocomposite materials with controlled ion mobilityk," ed: Wiley Online Library, 1995.

[17] J. Wang, J. Merino, P. Aranda, J.-C. Galván, and E. Ruiz-Hitzky, "Reactive nanocomposites based on pillared clays," *Journal of Materials Chemistry,* vol. 9, no. 1, pp. 161-167, 1999.

[18] E. . Ruiz-Hitzky, B. Casal, P. Aranda, and J. Galvän, "Inorganic-organic nanocomposite materials based on macrocyclic compounds," *Reviews in Inorganic Chemistry,* vol. 21, no. 1-2, pp. 125-159, 2001.
[19] M. L. Rojas-Cervantes, B. Casal, P. Aranda, M. Savirón, J. Galván, and E. Ruiz-Hitzky, "Hybrid materials based on vanadium pentoxide intercalation complexes," *Colloid and Polymer Science,* vol. 279, pp. 990-1004, 2001.
[20] L. Nicole, C. Boissière, D. Grosso, A. Quach, and C. Sanchez, "Mesostructured hybrid organic–inorganic thin films," *Journal of Materials Chemistry,* vol. 15, no. 35-36, pp. 3598-3627, 2005.
[21] A. Walcarius, D. Mandler, J. A. Cox, M. Collinson, and O. Lev, "Exciting new directions in the intersection of functionalized sol–gel materials with electrochemistry," *Journal of Materials Chemistry,* vol. 15, no. 35-36, pp. 3663-3689, 2005.
[22] J. C. Galván, P. Aranda, J. M. Amarilla, B. Casal, and E. Ruiz-Hitzky, "Organosilicic membranes doped with crown-ethers," *Journal of Materials Chemistry,* vol. 3, no. 6, pp. 687-688, 1993.
[23] P. Aranda, A. Jiménez-Morales, J. C. Galván, B. Casal, and E. Ruiz-Hitzky, "Composite membranes based on macrocycle/polysiloxanes: preparation, characterization and electrochemical behaviour," *Journal of Materials Chemistry,* vol. 5, no. 6, pp. 817-825, 1995.
[24] A. Abdraboh, A. A. Abdel-Aal, and K. T. Ereiba, "Preparation and characterization of inorganic organic hybrid material based on TEOS/MAPTMS for biomedical applications," *Silicon,* vol. 13, pp. 613-622, 2021.
[25] O. Lev *et al.*, "Sol− gel materials in electrochemistry," *Chemistry of Materials,* vol. 9, no. 11, pp. 2354-2375, 1997.
[26] B. Wang, B. Li, Q. Deng, and S. Dong, "Amperometric glucose biosensor based on sol− gel organic− inorganic hybrid material," *Analytical Chemistry,* vol. 70, no. 15, pp. 3170-3174, 1998.
[27] A. Walcarius, "Electrochemical applications of silica-based organic− inorganic hybrid materials," *Chemistry of Materials,* vol. 13, no. 10, pp. 3351-3372, 2001.
[28] T. N. Myasoedova, R. Kalusulingam, and T. S. Mikhailova, "Sol-gel materials for electrochemical applications: recent advances," *Coatings,* vol. 12, no. 11, p. 1625, 2022.
[29] M. Popall, M. Andrei, J. Kappel, J. Kron, K. Olma, and B. Olsowski, "ORMOCERs as inorganic–organic electrolytes for new solid state lithium batteries and supercapacitors," *Electrochimica acta,* vol. 43, no. 10-11, pp. 1155-1161, 1998.
[30] M. Zheludkevich, I. M. Salvado, and M. Ferreira, "Sol–gel coatings for corrosion protection of metals," *Journal of Materials Chemistry,* vol. 15, no. 48, pp. 5099-5111, 2005.
[31] V. Barranco, N. Carmona, J. Galván, M. Grobelny, L. Kwiatkowski, and M. Villegas, "Electrochemical study of tailored sol–gel thin films as pre-treatment prior to organic coating for AZ91 magnesium alloy," *Progress in Organic Coatings,* vol. 68, no. 4, pp. 347-355, 2010.
[32] M. J. Owen, "3-Methacryloxypropyltrimethoxysilane," *Progress in Silicones and Silicone-Modified Materials,* pp. 47-56, 2013.
[33] O.-H. Park, Y.-J. Eo, Y.-K. Choi, and B.-S. Bae, "Preparation and optical properties of silica-poly (ethylene oxide) hybrid materials," *Journal of sol-gel science and technology,* vol. 16, pp. 235-241, 1999.
[34] A. A. El Hadad, D. Carbonell, V. Barranco, A. Jiménez-Morales, B. Casal, and J. C. Galván, "Preparation of sol–gel hybrid materials from γ-methacryloxypropyltrimethoxysilane and tetramethyl orthosilicate: study of the hydrolysis and condensation reactions," *Colloid and polymer science,* vol. 289, pp. 1875-1883, 2011.
[35] P. Walker, "Silane and other adhesion promoters in adhesive technology," *Handbook of adhesive technology. New York: Taylor & Francis Group,* pp. 205-222, 2003.
[36] X. Lu, D. Chao, J. Chen, W. Zhang, and Y. Wei, "Preparation and characterization of inorganic/organic hybrid nanocomposites based on Au nanoparticles and polypyrrole," *Materials letters,* vol. 60, no. 23, pp. 2851-2854, 2006.
[37] L. C. U. Junqueira and J. Carneiro, *Basic histology: text & atlas*. McGraw-Hill New York, 2005.
[38] C.-I. Ilie *et al.*, "Decoration of a glass surface with AgNPs using thio-derivates for environmental applications," *Coatings,* vol. 14, no. 1, p. 96, 2024.
[39] A. A. Abdel-Aal, A. Abd Raboh, and K. Tohamy, "physical properties of (SiO2-CaCl2) doped with 3-methacryloxypropyl trimethoxysilane (MAPTMS)," *Egyptian Journal of Biomedical Engineering and Biophysics,* vol. 21, no. 1, pp. 65-73, 2020.
[40] J. P. Matinlinna, M. Özcan, L. V. Lassila, and P. K. Vallittu, "The effect of a 3-methacryloxypropyltrimethoxysilane and vinyltriisopropoxysilane blend and tris (3-trimethoxysilylpropyl) isocyanurate on the shear bond strength of composite resin to titanium metal," *Dental Materials,* vol. 20, no. 9, pp. 804-813, 2004.